International Journal of QUANTUM CHEMISTRY

A Road to a Multiconfigurational Ensemble Density Functional Theory without Ghost Interactions

Ewa Pastorczak and Katarzyna Pernal*

Ensemble density functional theory (DFT) is a theory potentially able to describe electronic states inaccessible to traditional time-dependent DFT approaches, e.g. Rydberg and double excitations. When combined with ensemble wavefunction approaches through a range-separation scheme of Stoll and Savin (Density Functional Methods in Physics, 1985, 177-207), a resulting multiconfiguration ensemble DFT is able to address also such challenging phenomena as bond breaking in the electronically excited molecules. Ensemble DFT is, however, crippled by the so-called "ghost interaction" error, analogous to the self-interaction error in the ground-state DFT. We are exploring ways to alleviate this effect. We also study the importance of spin polarization in the density functional, the self-consistency effects and the impact of tunable parameters on the quality of shapes of potential energy surfaces. © 2016 Wiley Periodicals, Inc.

DOI: 10.1002/qua.25107

Introduction

Among many methods of computing the electronic excitation energies of molecules the time-dependent density functional theory (TD DFT)[1] has become the most popular approach in the last decades. It happened mainly because of its relatively low computational cost, characterizing all DFT-based methods, and its good performance for valence excitations of single character. With this rise of popularity, however, also the failures of TD-DFT came to light, such as its inability to describe charge-transfer states,[2] excitations of multiple character,[3] and Rydberg excitations. On the other hand, the accurate, but computationally demanding *ab initio* methods are still limited to describing only small and medium-size systems. This seemingly stalemate situation has given an impulse to a certain renaissance of time-independent density functional theory-based methods of obtaining excitations energies. One group of methods belonging to this category is based on the idea of minimizing the energy of a single excited state of a certain symmetry[4] and in a more general approach of a state orthogonal to the ground state.[5] A related but more sophisticated approach to the problem of finding excitation energies within DFT is offered by a constrained-variational DFT.[6,7] Other approaches involve combining the density functional theory with perturbation theory[8,9] or with configuration interaction method.[10,11]

The last group of methods, the ensemble DFT, originates from the ensemble variational principle (EVP),[12] which states that a weighted sum of m lowest eigenvalues of the Hamiltonian is not greater than the weighted sum of m expectation values of this Hamiltonian with respect to any set of orthogonal wavefunctions, i.e.

$$\sum_{I=1}^{m} \omega_I E_I \leq \sum_{I=1}^{m} \omega_I \langle \Psi_I | \hat{H} | \Psi_I \rangle \tag{1}$$

provided that the weights fulfill a condition $0 \leq \omega_1 \ldots \leq \omega_m$. In the most straightforward approach, the EVP can be used to obtain the best "mean average" approximations of wavefunctions of the states belonging to the ensemble.[13,14] The EVP gained more attention, when based on it an ensemble density functional theory was proposed by Theophilou.[12] In the so-called "subspace density functional theory" equal weights were assumed and the energy functional was minimized to obtain the optimal ensemble electron density (i.e. a weighted sum of electron densities of states forming the ensemble). Introduction of the ensemble energy as a functional of the ensemble density was subsequently justified by a proof of an analog of the Hohenberg-Kohn theorem for the ensemble density.[15,16]

This new theory in principle capable of describing double excitations and potential energy surfaces became on object of extensive theoretical research[17–21] and a few numerical implementations.[21–24] Due to the lack of good approximation of the ensemble exchange-correlation functionals and the difficulties associated with imposing the orthogonality condition on the wavefunctions those realizations have been so far rather scarce and only moderately successful, apart from the pragmatic approach of Filatov and coworkers.[25,26]

In our previous work[27] we proposed two methods of calculation, based on the EVP. One method, called Ens-WF, is purely wavefunction-based and it is closely related to the state-averaged multiconfigurational self-consistent field (SA-MCSCF) method of Werner and Mayer.[28] Ens-WF consists in the optimization of the ensemble energy with respect to the orbitals and a subsequent diagonalization of the Hamiltonian in the basis of the Slater determinants included in the ensemble. To include the dynamic correlation in the description of the

E. Pastorczak, K. Pernal
Institute of Physics, Lodz University of Technology, Ul. Wolczanska 219, Lodz, 90-924, Poland
E-mail: pernalk@gmail.com, Fax: (+48) 426 313 639
Contract grant sponsor: National Science Centre of Poland; contract grant number: DEC-2012/05/B/ST4/01200.

states, we proposed a range-separated method[29] based on Ens-WF in which the short-range part of the electron-electron interaction is described by an ensemble density functional. Such a method, while describing well the lowest states in small molecules like LiH, was hampered by lack of spin polarization in the density-functional part, a so-called "ghost interaction," a well-known problem in the ensemble DFT,[19,21,30,31] and, in more general sense, the use of the ground-state density functionals for the description of excited states.[32] In Ref. [33], we proposed a solution to the first two problems and we explore this idea further in the present paper.

Theory

Throughout the article, a number of states will be denoted with *m*, the capital letters *I* and *J* will refer to states while *i*, *j* to orbitals. There exist two main approaches to obtaining excitation energies originating from the ensemble variational theory: (1) the purely wavefunction-based methods, exemplified by the ensemble Hartree-Fock (eHF) method or the aforementioned Ens-WF method, (2) the ensemble density functional theory in its different realizations. The Ens-WF method consists in a two-step minimization of the ensemble energy

$$E=\sum_{I=1}^{m}\omega_I\langle\psi_I|\hat{H}|\psi_I\rangle \quad . \tag{2}$$

In the first step the ensemble energy is minimized with respect to orbitals after assuming wavefunctions ψ_I's to be in a form of single-determinants $\{\Phi_I\}$. This leads to obtaining single-determinantal wavefunctions with optimal orbitals, $\{\Phi_J^{\mathrm{opt}}\}$. In the second step, a diagonalization of the Hamiltonian in the basis of those determinants is performed to obtain multiconfiguration wavefunctions

$$\psi_I=\sum_{J}^{m}C_{IJ}\Phi_J^{\mathrm{opt}} \quad , \tag{3}$$

which are employed to find the final ensemble energy (2). Such an approach is known to capture the static correlation and to produce fairly correct shapes of dissociation curves of small molecules. If an ensemble consisting of all possible configurations was used, Ens-WF would be equivalent to a Full Configuration Interaction method and the resulting ensemble energy (2) would be exact. For small ensembles, however, Ens-WF almost completely lacks the description of the dynamic correlation. On the other hand, approximate density functional methods based on a single-determinant description of states, while they usually account for the dynamic correlation, can only be used to describe molecules in their equilibrium geometries and excitations of single character.

For obtaining potential energy surfaces and capturing states of different characters, a multiconfigurational approach is needed. To retain the modest cost of the Ens-WF method, a range-separated scheme can be employed, within which long-range part of the electron-electron interaction is described by the wavefunction method, and the short-range part—by a density functional. Such an approach was proposed in Ref. [27]. In the Ens-lrWF + srDF method the electron-electron interaction operator is separated into a short- and a long-range part, i.e.[29]

$$\frac{1}{r}=v_{\mathrm{ee}}^{\mathrm{SR}}(r)+v_{\mathrm{ee}}^{\mathrm{LR}}(r) \quad , \tag{4}$$

such that $\lim_{r\to\infty} r\, v_{\mathrm{ee}}^{\mathrm{LR}}(r)=1$ and $\lim_{r\to 0} r\, v_{\mathrm{ee}}^{\mathrm{SR}}(r)=1$. Then, the universal functional of the ensemble density $\rho_{\mathrm{ens}}=\sum_{I=1}^{m}\omega_I\rho_I$ (where ρ_I represents density of the *I*-th state) defined as

$$F_{m,\omega}[\rho_{\mathrm{ens}}]=\min_{\substack{\{\psi_I\}\to\rho_{\mathrm{ens}}\\ \forall_{IJ}\ \langle\psi_I|\psi_J\rangle=\delta_{IJ}}}\sum_{I=1}^{m}\omega_I\langle\psi_I|\hat{T}+\hat{V}_{\mathrm{ee}}|\psi_I\rangle \quad , \tag{5}$$

can be partitioned into a long-range

$$F_{m,\omega}^{\mathrm{LR}}[\rho_{\mathrm{ens}}]=\min_{\substack{\{\psi_I\}\to\rho_{\mathrm{ens}}\\ \forall_{IJ}\ \langle\psi_I|\psi_J\rangle=\delta_{IJ}}}\sum_{I=1}^{m}\omega_I\langle\psi_I|\hat{T}+\hat{V}_{\mathrm{ee}}^{\mathrm{LR}}|\psi_I\rangle \tag{6}$$

and a short-range

$$F_{m,\omega}^{\mathrm{SR}}[\rho_{\mathrm{ens}}]=F_{m,\omega}[\rho_{\mathrm{ens}}]-F_{m,\omega}^{\mathrm{LR}}[\rho_{\mathrm{ens}}] \quad , \tag{7}$$

part. The ensemble energy expression then reads

$$E_{m,\omega}[\{\psi_I\}]=\sum_{I=1}^{m}\omega_I\langle\psi_I|\hat{T}+\hat{V}_{\mathrm{ee}}^{\mathrm{LR}}+\hat{V}_{\mathrm{ext}}|\psi_I\rangle+F_{m,\omega}^{\mathrm{SR}}[\rho_{\mathrm{ens}}] \quad . \tag{8}$$

If an exact short-range functional $F_{m,\omega}^{\mathrm{SR}}[\rho_{\mathrm{ens}}]$ was used, the resulting ensemble energy would be also exact. In the method Ens-lrWF + srDF, however, $F_{m,\omega}^{\mathrm{SR}}[\rho_{\mathrm{ens}}]$ is approximated by a ground-state short-range Hartree-exchange-correlation functional $E_{\mathrm{Hxc}}^{\mathrm{SR}}[\rho_{\mathrm{ens}}]$. To account for both dynamic and static correlation the Ens-lrWF + srDF method assumes (similarly to the Ens-WF approach presented earlier) two steps. First, the ensemble energy

$$E_{\mathrm{ens}}^{\mu\mathrm{GOK\text{-}DFT}}=\sum_{I=1}^{m}\sum_{i}^{M}\omega_I n_i^I h_{ii}+\frac{1}{2}\sum_{I=1}^{m}\sum_{i,j}^{M}\omega_I n_i^I n_j^I\langle ij||ij\rangle^{LR}+E_{\mathrm{Hxc}}^{\mathrm{SR}}[\rho_{\mathrm{ens}}] \tag{9}$$

is minimized with respect to the orbitals. In Eq. (9), *M* stands for a dimension of the spin orbital space, $\left\{\langle ij||ij\rangle^{LR}\right\}$ are antisymmetrized long-range two-electron integrals employing the interaction operator $\frac{\mathrm{erf}(\mu r)}{r}$ with a range-separation parameter μ, and n_i^I is the occupation number of the *i*th orbital in the *I*th single-determinant state, i.e.

$$n_i^I=\begin{cases}1 & i\in I\\ 0 & i\notin I\end{cases} \quad . \tag{10}$$

In the second step an effective Hamiltonian is diagonalized to obtain optimal wavefunctions. Such a simple approach is possible owing to employing short-range density functionals $E_{\mathrm{Hxc}}^{\mathrm{SR}}[\rho_{\mathrm{ens}}]$ dependent explicitly on the ensemble density which

ensures the existence of a short-range potential $V^{SR}_{m,\omega}[\rho_{ens}]$ common to all the orbitals and allows for the construction of an effective Hamiltonian. The final ensemble energy follows from taking the sum $\sum_{I=1}^{m}\omega_I\langle\psi_I|\hat{H}^{LR}|\psi_I\rangle$, computed with the multireference wavefunctions and adding a short-range ensemble energy $E^{SR}_{Hxc}[\rho_{ens}]$.

While Ens-lrWF + srDF has been shown to correctly describe dissociation curves of some small molecules (even using a small set of configurations), it has two major drawbacks. First is the obvious lack of spin polarization in the short-range part, which results in underestimating gaps between singlet and triplet states of the same spatial configurations. The other drawback is the "ghost-interaction" problem, that plagues the ensemble density functionals explicitly dependent on the ensemble density.

To resolve the first of the mentioned problems, namely the lack of spin polarization, the range-separated ensemble functional of the form (9) can be substituted by a functional

$$E^{\mu\text{spGOK-DFT}}_{ens}=\sum_{I=1}^{m}\sum_{i}^{M}\omega_I n_i^I h_{ii}+\frac{1}{2}\sum_{I=1}^{m}\sum_{i,j}^{M}\omega_I n_i^I n_j^I\langle ij||ij\rangle^{LR}+E^{SR}_{Hxc}\left[\rho^{\alpha}_{ens},\rho^{\beta}_{ens}\right], \tag{11}$$

with spin ensemble densities $\rho^{\sigma}_{ens}=\sum_I\omega_I\rho^{\sigma}_I$, $\sigma=\alpha,\beta$ computed by adding spin densities corresponding to each state $\rho^{\sigma}_I(x)=\sum_i^M n_i^I\,|\varphi_{i\sigma}(x)|^2$. In Eqs. (9) and (11), $\{h_{ij}\}$ denote one-electron integrals that contain contributions from the kinetic and external potential energy operators. It is worth noting that the range-separated functional of the form (9) contains already some spin polarization in its long-range (i.e. Hartree-Fock) part. This observation, together with large values of the range-separation parameter μ used in work[27] (corresponding to large contributions of the Hartree-Fock exchange) can explain relatively good results obtained by the method Ens-lrWF + srDF which employs the functional given in Eq. (9). However, to fully take into account the spin polarization, it is necessary to rather use the functional of the form (11). Unfortunately, there is a computational disadvantage related to such a choice. Namely, a short-range potential common to all states in the ensemble cannot be constructed so the optimization of the functional (11) cannot proceed via diagonalization of the effective Hamiltonian.

On the other hand, also the elimination of the "ghost interaction" error[19,30,31] has been shown to be best achieved by employing orbital-dependent functionals of the form

$$E^{\mu\text{-eDFT}}_{ens}=\sum_{I=1}^{m}\sum_{i}^{M}\omega_I n_i^I h_{ii}+\frac{1}{2}\sum_{I=1}^{m}\sum_{i,j}^{M}\omega_I n_i^I n_j^I\langle ij||ij\rangle^{\mathrm{LR}}+\sum_{I=1}^{m}\omega_I E^{SR}_{Hxc}[\rho_I] \tag{12}$$

and taking into account the spin polarization:

$$E^{\mu\text{-speDFT}}_{ens}=\sum_{I=1}^{m}\sum_{i}^{M}\omega_I n_i^I h_{ii}+\frac{1}{2}\sum_{I=1}^{m}\sum_{i,j}^{M}\omega_I n_i^I n_j^I\langle ij||ij\rangle^{\mathrm{LR}}+\sum_{I=1}^{m}\omega_I E^{SR}_{Hxc}\left[\rho^{\alpha}_I,\rho^{\beta}_I\right]. \tag{13}$$

The above form of the functional can be also seen as originating from the ensemble Hartree-Fock (eHF) functional, i.e.

$$E^{\mathrm{eHF}}_{ens}=\sum_{I=1}^{m}\omega_I\langle\Phi_I|\hat{H}|\Phi_I\rangle=\sum_{I=1}^{m}\sum_{i}^{M}\omega_I n_i^I h_{ii}+\frac{1}{2}\sum_{I=1}^{m}\sum_{i,j}^{M}\omega_I n_i^I n_j^I\langle ij||ij\rangle \tag{14}$$

where the dynamical correlation is accounted for by replacing two-electron integrals with their long-range counterpart and by adding the short-range Hartree-exchange-correlation functional. Similarly, the Ens-WF method described in Ref. [27] consisting in the minimization of the Eq. (14) with respect to the orbitals and then the diagonalization of the Hamiltonian in the basis of the determinants building the ensemble, can be viewed as the eHF method with static correlation added on top. The goal of creating a multiconfiguration ensemble method is to include all of the aforementioned features—the spin polarization, lack of the ghost-interaction error, and the description of the dynamic and static correlation. This is not a trivial task, especially if one wants to retain the favorable cost of the method, comparable to that of the ground-state DFT. In the next paragraphs we will show the route to constructing such a method, by building step by step more sophisticated methods based on Ens-WF. Later, on a few examples, we will show how each step of this sophistication influences the results.

First, and the most naive way to include the dynamic correlation is to use the range-separated expression for energy

$$E_{ens}=\sum_{I}^{m}\omega_I\left\{\sum_{JK}C^*_{IJ}C_{IK}\langle\Phi_J|\hat{H}^{\mathrm{LR}}|\Phi_K\rangle+E^{SR}_{Hxc}\left[\rho^{\alpha}_I,\rho^{\beta}_I\right]\right\} \tag{15}$$

with the dynamical correlation included through replacing the full-range electron interaction operator $(r_{12})^{-1}$ with its long-range counterpart and adding the short-range functional E^{SR}_{Hxc}. Notice that the difference with the functional used in the Ens-lrWF + srDF method is in the SR functional, which is now employed in a spin-polarized variant. The excitation energies can be extracted computing the ensemble energy derivatives with respect to the weights (or β parameter, see Ref. [32]), but in practice it is not a viable method. Instead, the approximate energy of the *I*-th state obtained with the Ens-WF method will be approximated using the optimal wavefunctions and the corresponding densities, as

$$E_I=\sum_{\mathrm{JK}}C^*_{IJ}C_{IK}\langle\Phi_J|\hat{H}^{\mathrm{LR}}|\Phi_K\rangle+E^{SR}_{Hxc}\left[\rho^{\alpha}_I,\rho^{\beta}_I\right]\ , \tag{16}$$

where $\rho^{\alpha}_I,\rho^{\beta}_I$ are spin densities computed for a multideterminant wavefunction $\Psi_I=\sum_J C_{IJ}\Phi_J$. We will discuss and test three computational algorithms based on Eqs. (15) and (16). The algorithms vary in a way how orbitals and the expansion coefficients C_{IJ} are obtained. In the first algorithm (called here Algorithm 1, *vide infra* for more detailed description) spin orbitals resulting from minimization of the eHF functional Eq. (14) are used and the expansion coefficients are obtained from diagonalization of the full-range Hamiltonian matrix. Such an approach has a modest computational cost and partly accounts for dynamical correlation, but neglects the influence of the correlation on the orbitals.

Algorithm 1

1. Build an ensemble of m Slater determinants (SD);
2. Assign fixed Boltzmann weights of the form

$$\omega_I = \frac{\exp\left[-\beta E_I\right]}{\sum_{K=1}^{m} \exp\left[-\beta E_K\right]} \tag{17}$$

   with approximate energies E_I computed for the equilibrium geometry to each SD.
3. Constrained (with orthogonality condition imposed on determinants) minimization of eHF energy Eq. (14) with respect to the orbitals;
4. Diagonalization of the full-range Hamiltonian matrix **H** (equivalent to minimizing the Ens-WF energy with respect to the C_{IJ} coefficients);
5. Computation of the state energies from Eq. (16).

To include the influence of the correlation on the orbitals, it is possible to minimize the energy (13) with respect to the orbitals. The subsequent diagonalization of the Hamiltonian matrix **H** no longer then minimizes the energy, but it provides one with pure-spin guesses for multiconfiguration wavefunctions. This method will be referred to as Algorithm 2.

Algorithm 2

1. Build an ensemble of m Slater determinants;
2. Assign Boltzmann weights to each SD;
3. Minimization of the ensemble energy (13) with respect to the orbitals;
4. Diagonalization of the full-range Hamiltonian **H** to obtain a guess for $\mathbb{C}$ matrix;
5. Computation of the states energies from Eq. (16).

The expansion coefficients $\{C_{IJ}\}$ can be also obtained by a direct optimization of the ensemble energy functional (15), under the constraint that the wavefunctions are orthogonal. Although it allows one to find a set of the optimal coefficients for a fixed set of the orbitals, such a minimization, without additional constraints, can lead to obtaining spin-contaminated wavefunctions. The corresponding method will be called Algorithm 3 in the rest of the work.

An obvious ultimate step—and as we will show later, an important one for the quality of the results—would be to perform the minimization of the ensemble energy with respect to the orbitals and the expansion coefficients self-consistently, while keeping the wavefunctions orthogonal and spin-adapted. This is, however, a complex computational task and has not been performed yet.

In short, in the Algorithm 1 the dynamic correlation is taken into account through the functional $E_{\mathrm{Hxc}}^{\mathrm{SR}}$ only in the energy expression (16) for a given state but not in the optimization steps. In the Algorithm 2, on the other hand, some additional part of the correlation is recovered through the self-consistent optimization of the orbitals with the short-range functional present in the energy expression. In addition, the Algorithm 3 should also offer a better description of the static correlation than the two simpler methods, because it leads to finding the optimal expansion coefficients $\{C_{IJ}\}$ (for the fixed orbitals).

Algorithm 3

1. Build an ensemble of m Slater determinants;
2. Assign Boltzmann weights to each SD;
3. Minimization of the ensemble energy (13) w.r.t. the orbitals;
4. Diagonalization of the full-range Hamiltonian to obtain a guess for $\mathbb{C}$ matrix;
5. Full optimization of the ensemble energy (15) w.r. t. the elements of $\mathbb{C}$;
6. Computation of the states energies from Eq. (16).

The expression (16) used to extract the energies of particular states is only rigorous in certain cases, e.g. for the range-separation parameter $\mu \to \infty$ the short-range functional tends to zero and the remaining part of the expression (16) provides a CI-type approximation to the excited state energy in question. For finite values of μ, Eq. (16) is just a practical and computationally efficient way of computing energies of states within a multiconfiguration ensemble DFT method which should serve as a reasonable approximation. While Franck and Fromager[32] proposed an expression involving a derivative of the ensemble energy with respect to a parameter defining the ensemble weights, this formula poses a difficult computational problem itself and it has not been yet used directly in any numerical implementation (although interpolation[34] and extrapolation[35] schemes were proposed to ease this task). What is more, the use of Eq. (16) lets one interpret the resulting wavefunctions as approximations to the true wavefunctions of the systems, which in turn allows for the interpretation of the character of particular excitations (e.g. if they are of single, double, valence or charge-transfer character). Such an interpretation means also, regrettably, that the quality of the resulting energies depends very strongly on the quality of obtained wavefunctions and their certain properties, like e.g. the spin symmetry.

Tests and Illustrative Examples

Computational details

The short-range exchange-correlation functional used for all presented computations is (restricted open-shell) short-range PBE.[36,37] Used benchmark values, basis sets and included configurations vary for different systems and are described within the text, but each time the set of configurations used was equal to the set of determinants corresponding to the states included in the ensemble (i.e. $m = M$). Boltzmann weights

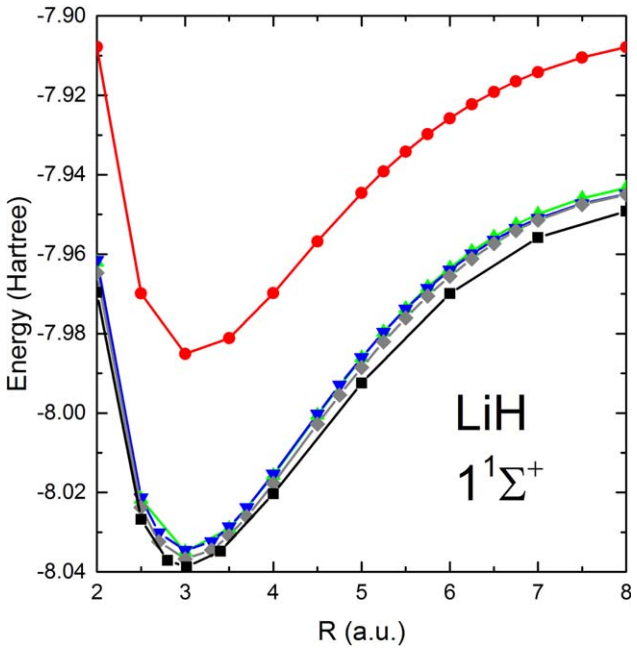

Figure 1. Dissociation curves of the ground state of LiH molecule. Circles ● denote Ens-WF, squares ■—LR-CCSD, triangles △—Algorithm 1, triangles ▽—Algorithm 2, diamonds ◇—Algorithm 3.

were computed with approximate state energies resulting from an eHF computation.

Homolytic dissociation

Dissociation curves of small molecules make particularly good models for studying the properties of computational methods for excited states, as they combine problems of bond breaking, single and double excitations and static correlation. At the same time, for small molecules such as presented here LiH, BH, H_2O, and N_2, accurate benchmark values of energies are available for comparison.

To analyze the influence of an inclusion of correlation at different levels (Ens-WF and Algorithms 1–3) on the energies of states of molecules, let us look at the energies of states of LiH molecule—$1^1\Sigma^+$ (the ground state, Fig. 1) and $1^3\Sigma^+$ (Fig. 2) along the dissociation curves. The ensemble used here contains configurations $\{1\sigma^2 2\sigma^2,\ 1\sigma^2 2\sigma 3\sigma,\ 1\sigma^2 3\sigma^2\}$ with all pertinent spin configurations. Calculations were performed in Aug-cc-pVDZ[38] basis set with β=0.5 [a parameter which determines the weights of states, see Ref. [27] and Eq. (17)] and $\mu = 1$ (the range-separation parameter). Reference energies were obtained with the LR-CCSD[39] method by employing DALTON[40] suite of programs. While the transition from Ens-WF method to the Algorithm 1 visibly lowers the absolute energies of both states, it does not change the shape of the curves. Clearly, the energies obtained with Algorithms 2 and 3 differ very little and the difference between the results produced by Algorithms 1 and 2 is practically invisible.

All three hybrid methods follow the LR-CCSD curves fairly well both in shape and in absolute values, with slight deviations for the ground-state in the dissociation limit and for the triplet in the mid-range limit. Overall, the methods in these case seem to give a well-balanced description of both the ground and the excited states. This is a typical example of how similar the outcomes of 2 and 3 actually are. In a few cases (especially for small values of μ), while the minimization of the ensemble energy with respect to the expansion coefficients would lower it by up to a few eV, at the same time it would introduce a severe breaking of the spin symmetry for some of the states (which has a negative impact on the shape of the dissociation curves). It becomes clear that the Algorithm 3 is not a good approximation to the self-consistent, multiconfiguration, ensemble-DFT-based method. Let us focus then on the two simpler Algorithms 1 and 2, which do not suffer from spin symmetry breaking.

BH molecule is a system very similar to LiH. Computations were performed in Aug-cc-pVTZ basis set and the configuration space consisted of 16 determinants constructed from the following configurations $\{1\sigma^2 2\sigma^2 3\sigma^2, 1\sigma^2 2\sigma^2 3\sigma 4\sigma,\ 1\sigma^2 2\sigma^2 3\sigma 1\pi, 1\sigma^2 2\sigma^2 4\sigma^2, 1\sigma^2 2\sigma^2 3\sigma 5\sigma\}$ with all pertinent spin combinations (except for $1\sigma^2 2\sigma^2 3\sigma 5\sigma$, where only the triplet was included).

The presented results from the ensemble calculations correspond to taking the range-separation parameter $\mu = 1$ and two values of the β parameter $\beta = 0$ and β=0.5. The results were compared with LR-CCSD energies calculated in the same basis set and energies obtained from a configuration interaction (CI) calculation performed in the same space as the ensemble calculation. Only a small difference between the performance of Algorithms 1 and 2 can be seen for $1^1\Sigma^+$ (i.e. the ground state, see Fig. 3) and $1^3\Sigma^+$ state (Fig. 4). The Algorithm 2, employing DFT orbitals produces for both states slightly lower energies. As expected, in an ensemble with dominant ground state (β=0.5, circle markers on Fig. 3) the ground state has a deeper minimum than in the equiensemble (see triangles on Fig. 3), at the expense of the description of $1^3\Sigma^+$ state

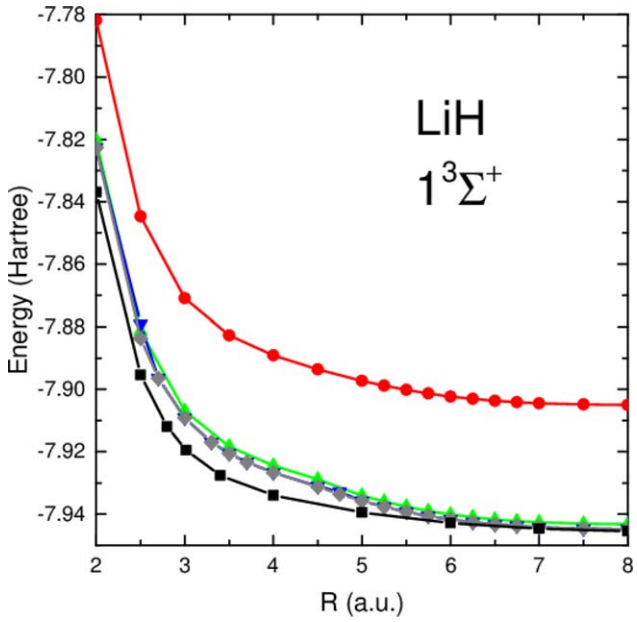

Figure 2. Dissociation curves of the first triplet state of LiH molecule. Circles ● denote Ens-WF, squares ■—LR-CCSD, triangles △—Algorithm 1, triangles ▽—Algorithm 2, diamonds ◇—Algorithm 3.

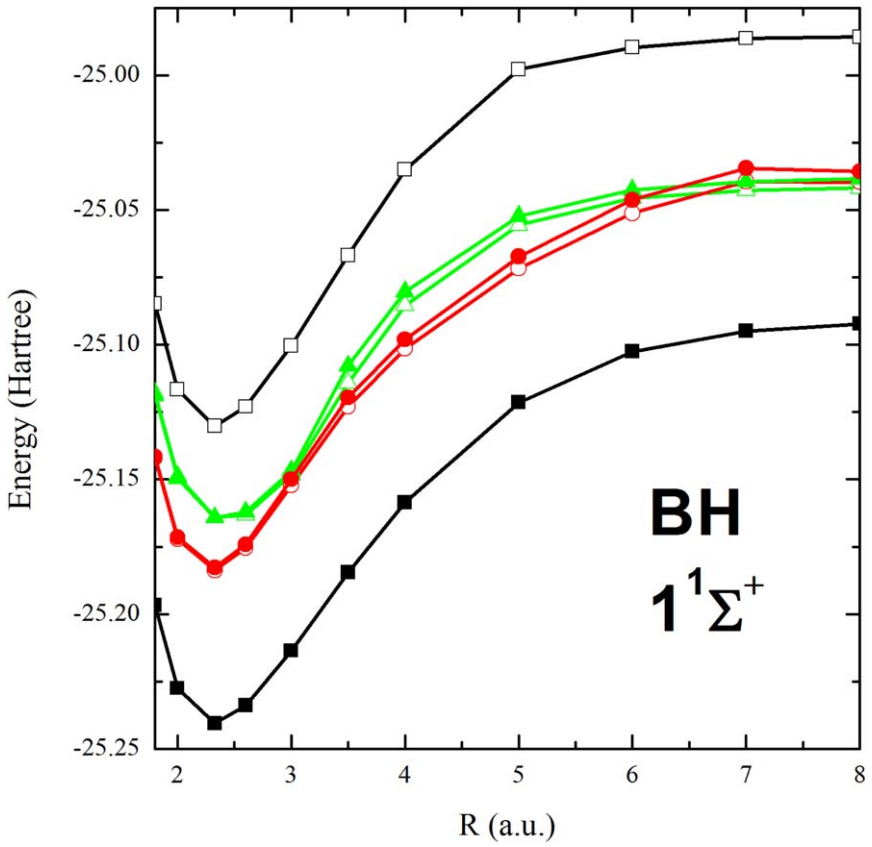

Figure 3. Dissociation curve of the ground state of BH molecule, $\mu = 1$. Empty squares (□) denote CI, full ones (■)—CCSD. Full circles ● denote β=0.5 Algorithm 1, empty circles ○—β=0.5, Algorithm 2. Full triangles ▲—$\beta = 0$, Algorithm 1, empty triangles △—$\beta = 0$, Algorithm 2.

(compare curves with circles vs. the one with triangles on Fig. 4). Our investigations, the results of which are only partly shown here, show that dependence of the quality of the results on β is rather random. For almost all states (bar $2^1\Sigma^+$, equiensemble case) significant improvement with respect to the CI method is achieved. Errors are reduced from hundreds of mHartree to tens of mHartree.

Finding an optimal value of the range-separation parameter μ was in the case of BH molecule a matter of compromise between the lowering effect of adding the dynamic correlation through the density functional and keeping the shapes of the dissociation curves correct through the wavefunction part. In the end, a value of $\mu = 1$ was chosen, as the lowest value that correctly reproduces the shape of dissociation curve of the state $2^1\Sigma^+$ (not shown here). In both figures for BH, Figures 3 and 4, it is clear that results obtained by the Algorithms 1 and 2 differ very little, similarly for Π states (not shown here). It is partially due to the choice of large value of μ which translates into a big contribution of eHF and, at the same time, small influence on the orbitals of the short-range functional in the Algorithm 2.

Stretching of the single O-H bond in a water molecule will shed more light on the performance of the methods. The calculations for H_2O were performed in Aug-cc-pVDZ basis set and the ensemble was built of configurations: $\{1a'^2 2a'^2 3a'^2 4a'^2 1a''^2$, $1a'^2 2a'^2 3a'^2 4a'5a'1a''^2$, $1a'^2 2a'^2 3a'^2 4a'^2 5a'1a''^2$, $1a'^2 2a'^2 3a'^2 4a'^2 5a'^2 1a''^2\}$ (a total of 13 determinants). The results were compared with CC3 energies calculated in the same basis set and energies obtained from a configuration interaction (CI) calculation performed in the same space as the ensemble calculation. For reasons that we will elaborate on in the following paragraphs we only show the equiensemble ($\beta = 0$) results.

As shown in Fig. 5, the results for the ground state obtained by Algorithms 1 and 2 are very similar, with a slightly deeper minimum produced by Algorithm 1. Both curves are much lower than the CI ones. They are qualitatively correct close to the dissociation limit, but they build a spurious maximum at R =3.5 a.u. and the minimum is still much too shallow. Both Algorithms 1 and 2 correctly reproduce the shape and the absolute energies of $1^3A'$ state (see Fig. 6). The CC3 benchmark is available only up to R=5.669 a.u., the calculations with this method diverge beyond that distance. It is known that the states $1^1A'$ and $1^3A'$ become degenerate in the dissociation limit and evidently both Algorithms 1 and 2 reproduce this behavior.

The energies of $1^1A''$ and $1^3A''$ states (Fig. 7) obtained with Algorithm 2 are satisfactory qualitatively and quantitatively. They are slightly higher than the CC3 benchmark, but the curves have correct shapes and the states become degenerate in the dissociation limit, as they should do. The energies of the $1^1A'$ state obtained with the Algorithm 1 are very similar to those obtained by means of the Algorithm 2, while the $1^3A''$ curve goes below the benchmark value and does not

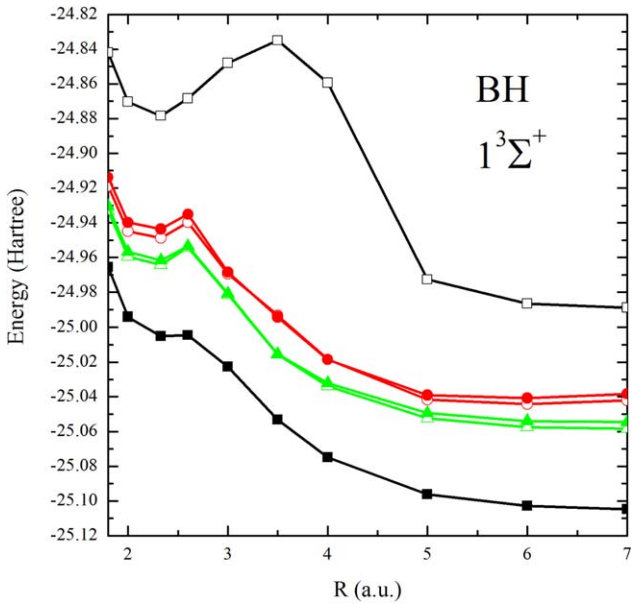

Figure 4. Dissociation curve of the $1^3\Sigma^+$ state of BH molecule $\mu = 1$. Empty squares (□) denote CI, full ones (■)—CCSD. Full circles ● denote β= 0.5 Algorithm 1, empty circles ○—β=0.5, Algorithm 2. Full triangles ▲—$\beta = 0$, Algorithm 1, empty triangles △—$\beta = 0$, Algorithm 2.

coincide with the $1^1A''$ state energy in the dissociation limit. The CI curves, on the other hand, are on average 300 mHartree higher than the ones obtained by Algorithms 1 and 2 and have incorrect shape.

Now, let us look at the most interesting state—the $2^1A'$ presented in Fig. 8. The curious behavior of this state is the reason why only the equiensemble results are shown. Only in proximity of $\beta = 0$ the shape of the curve is approximately correctly reproduced. This phenomenon owes to the fact that the virtual orbitals obtained from a ground-state HF computation

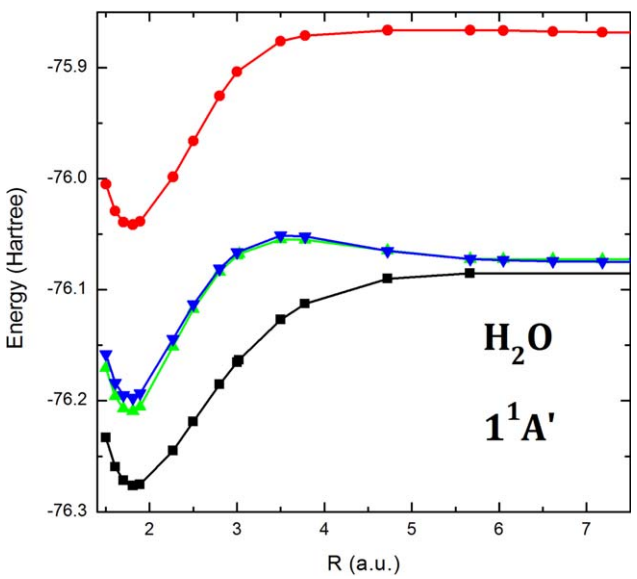

Figure 5. Dissociation curve of the ground state of H_2O molecule, $\mu = 1$, $\beta = 0$. Symbols ■ denote CC3 results, ●—CI β=0.5, ▲—Algorithm 1, ▼—Algorithm 2.

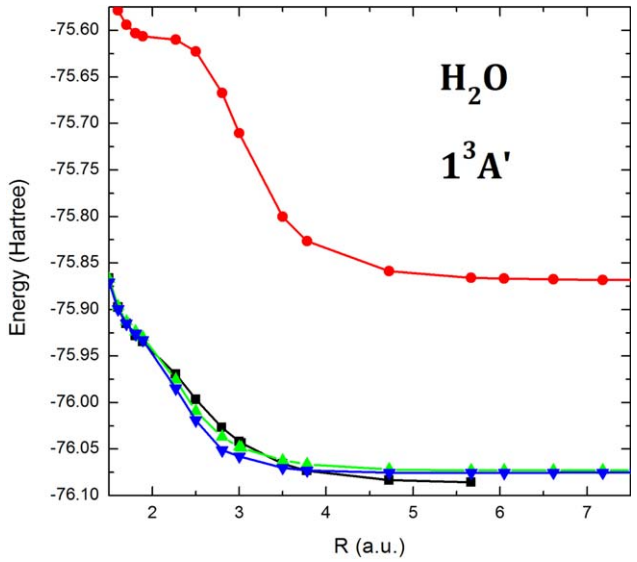

Figure 6. Dissociation curve of the $1^3A'$ state of H_2O molecule, $\mu = 1$, $\beta = 0$. Symbols ■ denote CC3 results, ●—CI $\beta = 0$, ▲—Algorithm 1, ▼—Algorithm 2.

(which corresponds to $\beta \to \infty$ in the eHF method) describe the $2^1A'$ state very poorly. In an equiensemble calculation $5a'$ orbital enters the optimization with a significant weight, which changes the shape of the dissociation curve of not only the $2^1A'$ state, but also $1^1A''$ and $1^3A''$ (cf. CI and Algorithm 2 curves in Figs. 7 and 8). MCSCF results (computed in Molpro[41,42] software package, with 65 configuration state functions) shown in Fig. 8 support this claim. When the orbitals are only optimized with respect to the ground state (CASSCF[43,44] in a minimal active space, single iteration), the curve is very erratic. Then, when the $2^1A'$ state is taken into account (SA-MCSCF in the same active space, with equal weights for the ground and the $2^1A'$ state, single iteration), the curve follows the ones

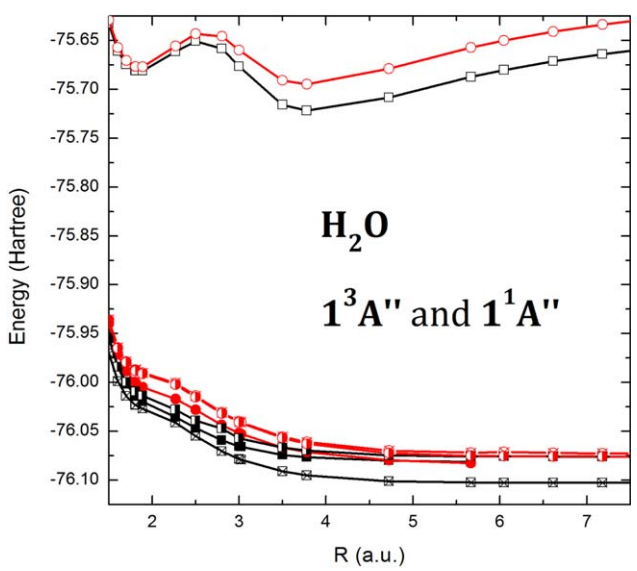

Figure 7. Dissociation curve of the $1^3A''$ and $1^1A''$ states of H_2O molecule, $\mu = 1$, $\beta = 0$. Squares denote $1^3A''$ state, circles—$1^1A''$, full symbols—CC3, empty—CI, half-filled—Algorithm 2, crossed—Algorithm 1.

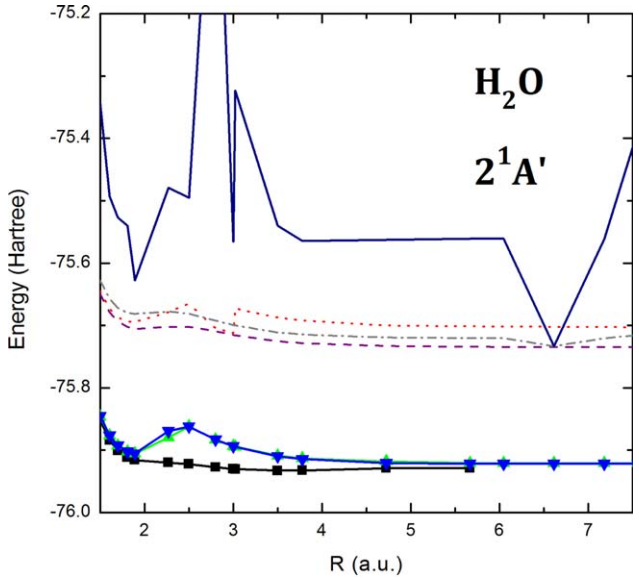

Figure 8. Dissociation curve of the $2^1A'$ state of H_2O molecule, $\mu = 1$, $\beta = 0$. Symbols ■ denote CC3 results, ▲—Algorithm 1, ▼—Algorithm 2, dashed line (- -)—SA-MCSCF, dash-dot (-·-)—CAS-SCF, dotted (· · ·)—SA-MCSCF with single iteration and solid line—CAS-SCF with single iteration.

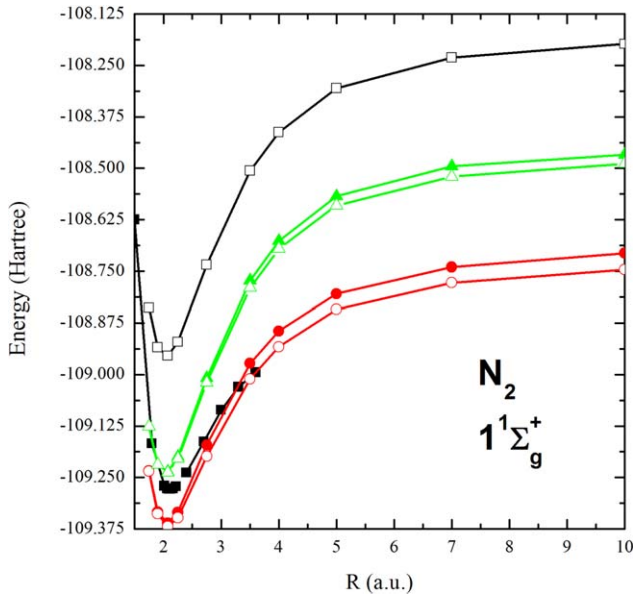

Figure 9. Dissociation curve of the ground state of N_2 molecule, $\beta = 0$. Symbols: full squares (■) denote FCI results, empty ones (□)—CI. Empty triangles (△) denote Algorithm 2, $\mu = 1$, full triangles (▲)—Algorithm 1, $\mu = 1$. Full circles (●)—Algorithm 1,μ=0.5, empty ones (○)—Algorithm 2, μ=0.5.

produced by the Algorithms 1 and 2. Still, spurious extrema are visible. Performing a self-consistent calculation (CASSCF or SA-MCSCF) then eliminates the spurious extrema and the shape of the curves is in good agreement with the one obtained with CC3, while the total energies remain significantly too high. This observation suggests that also a multi-configuration ensemble DFT, if implemented self-consistently, would produce the curves of correct shape. The behavior of this state is a good illustration of the impact the self-consistency has on the solution—while the short-range density-functional is alleviating the method's sensitivity to the size of the active space, the self-consistency is often essential for producing orbitals of sufficient quality. Still, the H_2O results are rather accurate, with the exception of the ground state. In that case, lower energies could of course be obtained with a larger value of β, but then the shape of $2^1A'$ state dissociation curve would deteriorate.

Another studied system was an N_2 molecule, stretched along its triple bond. The calculations were performed in cc-pVDZ basis set. The singlet state energies were compared with FCI results[45] while the triplet state with the CC3 results computed in the same basis set. The ensemble included 12 determinants. In the case of N_2 the value of β seems to have very little influence on the results, so only the results for the equi-ensemble results are presented. The shapes of the curves obtained with Algorithms 1 and 2 are very similar to the CI ones, which means that the orbitals from ensemble calculations are similar to the Hartree-Fock ones.

Already by looking at Fig. 9 one concludes that the method struggles with N_2. Even though by tuning the μ parameter one could obtain a good agreement of the Algorithm 2 (or Algorithm 1) with the FCI benchmark in the minimum but the energy rises too steeply with the bond length. It suggests (and is indeed confirmed by work[45]) that for medium and large distances the contribution of triply excited determinants is significant. This leads us to belief that the problem could only be remedied by expanding the ensemble.

One can make the same conclusions about the first excited state (Fig. 10). Larsen et al.[45] also in this case mention large contribution of multiply excited determinants for larger bond lengths. Unfortunately, no FCI benchmark for triplet states of N_2 is available, so employ the CC3 results as reference. As Larsen et al. mention, CC3 model is reliable for small distances,

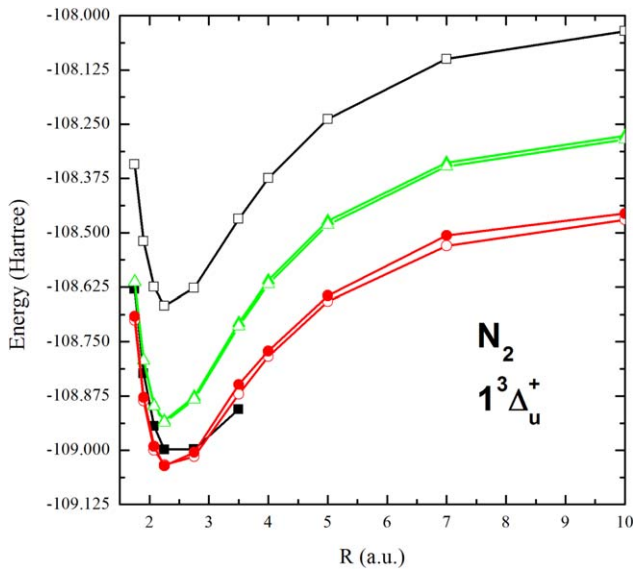

Figure 10. Dissociation curve of the $1^3\Delta$ state of N_2 molecule, $\beta = 0$. Symbols: full squares (■) denote CC3 results, empty ones (□)—CI. Empty triangles (△) denote Algorithm 2, $\mu = 1$, full triangles (▲)—Algorithm 1, $\mu = 1$. Full circles (●)—Algorithm 1, μ=0.5, empty ones (○)—Algorithm 2, μ=0.5.

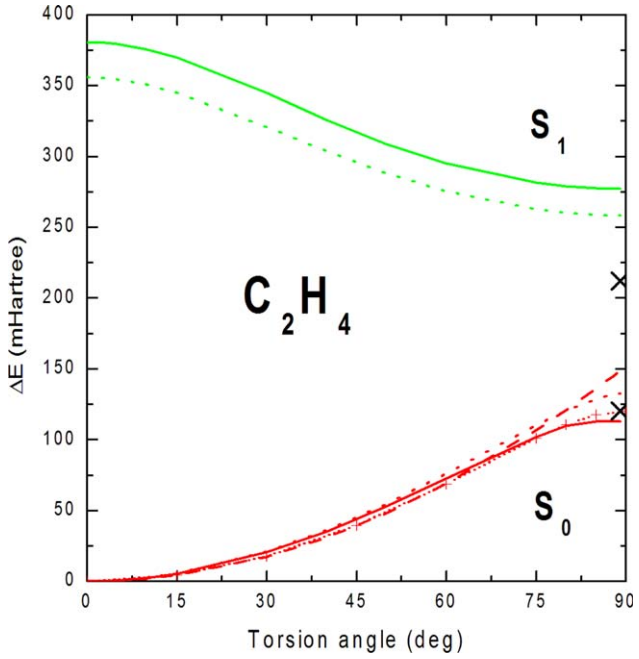

Figure 11. Torsion of C_2H_4 molecule, $\beta = 1$, $\mu = 1$. Dotted lines—CI method, dashed lines—ground state PBE, solid lines—Algorithm 1, dashes and crosses—TCSCF-CISD[46] (benchmark), black crosses—experimental gap.[47]

but tends to overestimate the correlation contribution for larger ones. We find that the $1^3\Pi$ state (not shown here) is very well-described near the minimum by the Algorithm 1 for the value of $\mu = 1$ with the error with respect to the CC3 benchmark at the minimum amounting to 1 mHa, which is also optimal for the singlets (the errors being equal to 40 mHa and 11 mHa for $1^1\Sigma_g^+$ and $1^1\Pi_g^+$, states, respectively), whereas the minimum of $1^3\Delta$ state (error of 62 mHa) is too shallow for this value of μ and only for μ=0.5 good agreement (error of 38 mHa) is obtained. It would be interesting to see the same computations performed for a larger basis set, unfortunately cc-pVDZ is the largest basis set for which a benchmark is available.

Torsion of ethylene

Finally, we test the Algorithm 1 with parameters identified as appropriate for most of the systems—$\mu = 1$ and $\beta = 1$ on a challenging case of twisting of the double bond of the ethylene molecule. Here, both the description of the ground state and the first excited singlet—which become nearly degenerate at 90° rotation angle—requires a multireference approach.

Table 1. The ground-state energy of ethylene (in Hartree), the barrier of rotation and relative energies of the first excited singlet state at 0° and 90° in mHartree. Computations with DZP basis set.[46]

	TCSCF-CISD[46]	Exp.[47]	Alg. 1	PBE	CI
S_0 energy	−78.366	–	−78.314	−78.476	−78.063
Barrier	120	103	112	149	133
ΔE (0°)	–	282	380	–	359
ΔE (90°)	–	202	277	–	258

Configurations included in the ensemble were $\{1a^22a^23a^21b_3^22b_3^21b_2^21b_1^2,\ 1a^22a^23a^21b_3^22b_32b_21b_1^2,\ 1a^22a^23a^21b_3^22b_21b_1^2\}$ and all computations were performed with DZP[46] basis set. As shown in Figure 11, the Algorithm 1 describes very well the ground state for all torsion angles, following closely the reference curve. The torsion barrier is closer to the experiment value than even the benchmark TCSCF-CISD result and the total ground-state energy also agrees very well with the TCSCF-CISD one (see Table 1). Ensemble method does not produce a cusp at 90° like the ground-state DFT (PBE functional) does. The description of the excited state is not as perfect. The curves produced by both CI and the ensemble method are systematically too high, which suggests that while the size of the ensemble is sufficient, the description suffers from the lack of full self-consistency. Regardless, the obtained result shows that the presented multiconfiguration ensemble method is able to reproduce the orthogonalization of ethylene.

Conclusions

We have investigated a hierarchy of multiconfiguration ensemble DFT methods based on the range-separated ensemble energy functional given in Eq. (15). The considered variants differ by the level of approximation with which the orbitals and the expansion coefficients entering Eq. (16) used to predict energies of different states are obtained. The multiconfiguration ensemble DFT approach avoids the problem of the spurious ghost interaction and takes into account spin polarization in the density functional part. The obtained results lead to the conclusion that the method in general is capable of reproducing the shapes of potential energy surfaces of ground and of excited states on equal footing. While in a longer perspective it seems necessary to introduce a fully self-consistent, spin-adapted method, at present the two simpler of the presented approaches—the Algorithms 1 and 2 produce the results of very similar quality, and they are more reliable than the more computationally costly Algorithm 3. The Algorithm 1, in which a range-separated functional is only used to compute the energies of states, may be preferable due to its very low computational cost and better stability.

At present the choice of the configurations included in the ensemble and of the optimal values of the range-separation and the weights-governing parameters, μ and β, respectively, is essential for the quality of the results. We anticipate, though, that upon introducing the full self-consistency the dependence of the results on the value of β will become less important.

The employed scheme of computing the energies according to Eq. (16) is a computationally robust and a pragmatic choice. It allows one to associate the computed energies with states of a given spin and spatial symmetry, which greatly improves the usefulness of the method. It has to be noted, however, that very recently an alternative approach to the ghost-interaction-free multiconfiguration ensemble DFT has been hinted in Ref. [35], but since neither the algorithm nor numerical examples were shown, it is difficult to assess the viability of this approach.

Keywords: ensemble density functional theory · excitation energy · range-separated functional

How to cite this article: E. Pastorczak, K. Pernal. *Int. J. Quantum Chem.* **2016**, *116*, 880–889. DOI: 10.1002/qua.25107

[1] M. Casida, *Recent Developments and Applications of Modern Density Functional Theory*, Vol. *4*; Elsevier, Amsterdam, **1996**.
[2] A. Dreuw, M. Head-Gordon, *J. Am. Chem. Soc.* **2004**, *126*, 4007.
[3] J. Neugebauer, E. J. Baerends, M. Nooijen, *J. Chem. Phys.* **2004**, *121*, 6155.
[4] T. Ziegler, A. Rauk, E. J. Baerends, *Theor. Chim. Acta* **1977**, *43*, 261.
[5] F. A. Evangelista, P. Shushkov, J. C. Tully, *J. Phys. Chem. A* **2013**, *117*, 7378.
[6] T. Ziegler, M. Seth, M. Krykunov, J. Autschbach, F. Wang, *J. Chem. Phys.* **2009**, *130*, 154102.
[7] I. Seidu, M. Krykunov, T. Ziegler, *Mol. Phys* **2014**, *1*, 661.
[8] A. Görling, *Phys. Rev. A* **1996**, *54*, 3912.
[9] E. Rebolini, J. Toulouse, A. M. Teale, T. Helgaker, A. Savin, *J. Chem. Phys.* **2014**, *141*, 044123.
[10] S. Grimme, M. Waletzke, *J. Chem. Phys.* **1999**, *111*, 5645.
[11] E. Rebolini, J. Toulouse, A. M. Teale, T. Helgaker, A. Savin, *Phys. Rev. A* **2015**, *91*, 032519.
[12] A. K. Theophilou, *J. Phys. C* **1979**, *12*, 5419.
[13] N. I. Gidopoulos, A. K. Theophilou, *Philos. Mag. B* **1994**, *69*, 1067.
[14] T. A. Kaplan, P. N. Argyres, *Ann. Phys.* **1975**, *92*, 1.
[15] E. K. U. Gross, L. N. Oliveira, W. Kohn, *Phys. Rev. A* **1988**, *37*, 2809.
[16] E. S. Kryachko, *Int. J. Quantum Chem.* **2005**, *103*, 818.
[17] F. Tasnadi, A. Nagy, *J. Chem. Phys.* **2003**, *119*, 4141.
[18] A. Nagy, *J. Phys. B* **2001**, *34*, 2363.
[19] N. I. Gidopoulos, P. G. Papaconstantinou, E. K. U. Gross, *Phys. Rev. Lett.* **2002**, *88*, 033003.
[20] Z. Yang, J. R. Trail, A. Pribram-Jones, K. Burke, R. J. Needs, C. A. Ullrich, *Phys. Rev. A* **2014**, *90*, 042501.
[21] A. Pribram-Jones, Z. Yang, J. R. Trail, K. Burke, R. J. Needs, C. A. Ullrich, *J. Chem. Phys.* **2014**, *140*, 18A541.
[22] V. N. Glushkov, A. K. Theophilou, *J. Phys. B* **2002**, *35*, 2313.
[23] I. Andrejkovics, A. Nagy, *Chem. Phys. Lett.* **1998**, *296*, 489.
[24] E. K. U. Gross, L. N. Oliveira, W. Kohn, *Phys. Rev. A* **1988**, *37*, 2821.
[25] A. Kazaryan, J. Heuver, M. Filatov, *J. Phys. Chem. A* **2008**, *112*, 12980.
[26] M. Filatov, *WIRES Comput. Mol. Sci.* **2015**, *5*, 146.
[27] E. Pastorczak, N. I. Gidopoulos, K. Pernal, *Phys. Rev. A* **2013**, *87*, 062501.
[28] H. J. Werner, W. Meyer, *J. Chem. Phys.* **1981**, *74*, 5794.
[29] H. Stoll and A. Savin, In *Density Functional Methods in Physics*; R. M. Dreizler, J. da Providencia, Eds.; Plenum, New York, **1985**; pp. 177–207.
[30] F. Tasnadi, A. Nagy, *J. Phys. B* **2003**, *36*, 4073.
[31] E. Pastorczak, K. Pernal, *J. Chem. Phys.* **2014**, *140*, 18A514.
[32] O. Franck, E. Fromager, *Mol. Phys.* **2014**, *112*, 1684.
[33] K. Pernal, N. I. Gidopoulos, E. Pastorczak, *Adv. Quantum Chem.* **2016**, *73*, 199.
[34] B. Senjean, S. Knecht, H. J. A. Jensen, E. Fromager, *Phys. Rev. A* **2015**, *92*, 012518.
[35] B. Senjean, E. D. Hedegård, M. Alam, S. Knecht, E. Fromager, *et al*. arXiv Preprint **2015**, arXiv, 1509.08033.
[36] J. P. Perdew, K. Burke, M. Ernzerhof, *Phys. Rev. Lett.* **1996**, *77*, 3865.
[37] E. Goll, M. Ernst, F. Moegle-Hofacker, H. Stoll, *J. Chem. Phys.* **2009**, *130*, 234112.
[38] T. H. Dunning, *J. Chem. Phys.* **1989**, *90*, 1007.
[39] H. Sekino, R. J. Bartlett, *Int. J. Quantum Chem.* **1984**, *26*, 255.
[40] Dalton, A Molecular Electronic Structure Program, Release 2.0, **2005**. Available at: http://www.kjemi.uio.no/software/dalton/dalton.html.
[41] H. J. Werner, P. J. Knowles, G. Knizia, F. R. Manby, M. Schütz, *WIRES Comput. Mol. Sci.* **2012**, *2*, 242.
[42] H.-J. Werner, P. J. Knowles, G. Knizia, F. R. Manby, M. Schütz, P. Celani, T. Korona, R. Lindh, A. Mitrushenkov, G. Rauhut, K. R. Shamasundar, T. B. Adler, R. D. Amos, A. Bernhardsson, A. Berning, D. L. Cooper, M. J. O. Deegan, A. J. Dobbyn, F. Eckert, E. Goll, C. Hampel, A. Hesselmann, G. Hetzer, T. Hrenar, G. Jansen, C. Köppl, Y. Liu, A. W. Lloyd, R. A. Mata, A. J. May, S. J. McNicholas, W. Meyer, M. E. Mura, A. Nicklass, D. P. O'Neill, P. Palmieri, D. Peng, K. Pflüger, R. Pitzer, M. Reiher, T. Shiozaki, H. Stoll, A. J. Stone, R. Tarroni, T. Thorsteinsson, M. Wang, Molpro, Version 2012.1, A Package of Ab Initio Programs; Cardiff, UK, **2012**. Available at: http://www.molpro.net
[43] P. J. Knowles, H. J. Werner, *Chem. Phys. Lett.* **1985**, *115*, 259.
[44] H. J. Werner, P. J. Knowles, *J. Chem. Phys.* **1985**, *82*, 5053.
[45] H. Larsen, J. Olsen, P. Jørgensen, O. Christiansen, *J. Chem. Phys.* **2000**, *113*, 6677.
[46] A. I. Krylov, D. C. Sherrill, *J. Chem. Phys.* **2002**, *116*, 3194.
[47] P. Foo, K. Innes, *J. Chem. Phys.* **1974**, *60*, 4582.

Received: 17 November 2015
Revised: 20 January 2016
Accepted: 22 January 2016
Published online 19 February 2016